Clinical Neurophysiology 130 (2019) 352–358

Contents lists available at ScienceDirect

Clinical Neurophysiology

journal homepage: www.elsevier.com/locate/clinph

From research to clinic: A sensor reduction method for high-density EEG neurofeedback systems

Prasanta Pal *, Daniel L. Theisen, Michael Datko, Remko van Lutterveld, Alexandra Roy, Andrea Ruf, Judson A. Brewer

Center for Mindfulness, University of Massachusetts Medical School, 222 Maple St., Shrewsbury, MA 01545, USA

ARTICLE INFO

Article history:
Accepted 22 November 2018
Available online 16 December 2018

Keywords:
Monte Carlo
EEG montage
Sensor reduction
Neurofeedback
Translational
Source localization

HIGHLIGHTS

- Introduces an adaptable method for targeted EEG sensor reduction using Monte Carlo sampling.
- Reliably reduced a 128-sensors source-space EEG neurofeedback system to 32-sensors.
- Reduced-sensors montages could reproduce 128-sensors feedback with high accuracy and design goals.

ABSTRACT

Objective: To accurately deliver a source-estimated neurofeedback (NF) signal developed on a 128-sensors EEG system on a reduced 32-sensors EEG system.
Methods: A linearly constrained minimum variance beamformer algorithm was used to select the 64 sensors which contributed most highly to the source signal. Monte Carlo-based sampling was then used to randomly generate a large set of reduced 32-sensors montages from the 64 beamformer-selected sensors. The reduced montages were then tested for their ability to reproduce the 128-sensors NF. The high-performing montages were then pooled and analyzed by a k-means clustering machine learning algorithm to produce an optimized reduced 32-sensors montage.
Results: Nearly 4500 high-performing montages were discovered from the Monte Carlo sampling. After statistically analyzing this pool of high performing montages, a set of refined 32-sensors montages was generated that could reproduce the 128-sensors NF with greater than 80% accuracy for 72% of the test population.
Conclusion: Our Monte Carlo reduction method was used to create reliable reduced-sensors montages which could be used to deliver accurate NF in clinical settings.
Significance: A translational pathway is now available by which high-density EEG-based NF measures can be delivered using clinically accessible low-density EEG systems.

1. Introduction

Neurofeedback (NF) helps users to induce behavioral change by presenting them with real-time feedback about their brain activity patterns. This method has seen wide success as a therapeutic tool for the treatment of ADHD, epilepsy, and addiction disorders (Lubar et al., 1995; Peniston and Kulkosky, 1991; Sterman and Egner, 2006). As the technology advances, NF is also now beginning to find applications in the commercial world. (Jatupaiboon et al., 2013; Jiang et al., 2016; Niha and Banu, 2016; Stytsenko et al., 2011; Surangsrirat and Intarapanich, 2015; Wu and Liou, 2015).

Currently, the majority of NF measures are being developed using low-density EEG (l-EEG) systems which consist of fewer than thirty-two electrodes (Niha and Banu, 2016). These systems are inexpensive and flexible, but the range of NF measures they can generate is constrained by their inability to measure highly complex and region-specific brain activity (Chu, 2015, Thibault et al.,

Abbreviations: NF, neurofeedback; l-EEG, low-density EEG; h-EEG, high density EEG; PCC, Posterior Cingulate Cortex; MC, Monte Carlo.

* Corresponding author.
E-mail address: Prasanta.Pal@umassmed.edu (P. Pal).

https://doi.org/10.1016/j.clinph.2018.11.023
1388-2457/

2016). In contrast, expensive high-density EEG (h-EEG) systems can measure a much broader range of brain activity and provide spatial resolutions high enough to allow for accurate source localization (Acar and Makeig, 2013). These capabilities enable h-EEG systems to produce a diverse range of NF measures (e.g. source signal, brain network integration etc.) that are currently inaccessible to their l-EEG counterparts.

Despite the unique advantages of h-EEG, such systems are rarely used for the development of NF measures. Due to their high purchasing costs, time-consuming complex setup procedures, and computational costs associated with high-dimensional data (Anderson, 1993), h-EEG systems are poorly suited for real world clinical and commercial applications (Chu, 2015; Mihajlović et al., 2015). Since NF research aims to develop clinically relevant tools, this makes h-EEG impractical for NF development without a translational pathway for implementing h-EEG NF measures on l-EEG systems. One way this translational pathway could be created is through the development of EEG sensor reduction techniques.

Although sensor reduction techniques played an important role in closely related sensor-driven medical imaging fields (Machado et al., 2018; Pellegrino et al., 2016), the literature on EEG sensor reduction is sparse and we are aware of only one other paper that attempts it. Herta and colleagues (Herta, et al., 2017) reduced an epilepsy detection system from 19 to 10 electrodes by an automated algorithm. They measured the performance of their algorithm against two human experts who identified seizure-related patterns in EEG data from epilepsy patients and found reduced-sensors arrays for which the algorithm identified similar patterns with high sensitivity and specificity. While this reduction strategy is useful for small EEG systems, its reliance on expert opinion and a well characterized target signal limit its applicability to larger, more complex EEG systems and signal patterns.

In the present work, we used a novel sensor reduction method to implement a source-estimated h-EEG NF signal on a reduced 32-sensors system (van Lutterveld et al., 2016). We used Monte Carlo-based (MC) sampling (Pal et al., 2008; Rubinstein and Kroese, 2016) to randomly generate a large set of reduced-sensors montage candidates. Montages in this random set were then rapidly screened for their ability to reproduce feedback similar to the full h-EEG sensors montage. The high-performing montages were then pooled and analyzed using various statistical methods (e. g. k-means cluster machine learning) to produce an optimized reduced montage. The aim of this paper was to establish a generic data-driven method which would enable h-EEG NF measures to be implemented on clinically accessible l-EEG systems.

2. Materials and methods

2.1. EEG data acquisition

A schematic diagram of the NF data collection procedure is illustrated in Fig. 1. High density EEG data used for the present study was collected from $n = 72$ subjects. The study was approved by the University of Massachusetts Medical School Institutional Review Board and all participants were provided a fact sheet before participation in the study. The NF they received was generated based on estimated Posterior Cingulate Cortex (PCC) activity and was presented as a meditation training tool similar to van Lutterveld et al. (2016). Each participant received 5 sessions of NF divided up over 5 weeks. Each of these sessions consisted of six, 4-min NF runs, during which the first 20 s were a baseline word task.

The NF time series presented to each participant in the form of audio feedback updated every two seconds, were derived from

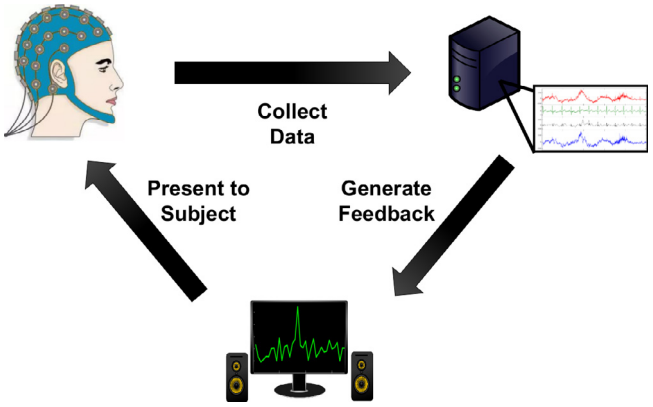

Fig. 1. Experimental setup for real-time neurofeedback. Data is collected from the subject and processed in real-time to generate a target neurofeedback signal. The signal is then presented back to the subject through an audio-visual interface.

gamma band (40–57 Hz) activity of the PCC using a linearly constrained minimum variance (LCMV) beamformer algorithm (Greenblatt et al., 2005). For additional details of the NF setup see van Lutterveld et al. (2016). The bandpass filter was implemented with a 2nd order IIR butterworth filter. The NF time series of each 4-min run were average-referenced and divided into 1-s epochs. Within each of these epochs, the gamma amplitude for this source-estimated PCC signal was averaged, smoothed using a half-Gaussian filter. The smoothed signal from each epoch was then presented to the subject in the form of a time series plot after each NF run. All subsequent analyses are based on the raw EEG data recorded from a Biosemi activetwo EEG system consisting of 128 active electrodes, collected at a sampling rate of 2048 Hz (Biosemi, 2011).

2.2. Sensor reduction

The goal of this sensor reduction method was to produce a set (Σ) of 32-sensor EEG montages which could reliably reproduce the NF signal generated by a 128-sensor EEG system. The selection of 32 reduced-sensors provides a good balance between signal robustness, ease of EEG setup, and wide clinical and commercial availability. In early testing of montages below 32-sensors, we found a significant (near exponential) drop off in average ρ values as well as rapid reduction in volume of the high correlation montage pool. As a matter of principle, a smaller montage size could have been generated, but would have required computational resources deemed unnecessary for this proof-of-concept article.

One major barrier to the construction of Σ is the "curse of dimensionality" (Friedman, 1997; Keogh and Mueen, 2011). In the context of this study, there is a vast number of 32-sensor montages that could be generated by randomly selecting sensors from the 128-sensors configuration space. Specifically, the 128-sensor configuration space Ω contains about 1.48×10^{30} 32-sensor montage combinations. The enormous volume of montages in Ω makes the use of exhaustive search algorithms computationally impractical for the discovery of high-performing montages.

As a more feasible approach, we developed a Monte Carlo (MC) sampling strategy which allows us to randomly, but uniformly, sample the entire 128-sensor configuration space. Because it can be safely assumed that a large number of montages in Ω are redundant, asymptotically convergent trends, if any, should emerge without the need to exhaustively explore Ω. These convergent trends should be attainable in a reasonable amount of time by using commercially available computational resources. An overview of our sensor reduction approach can be seen in Fig. 2.

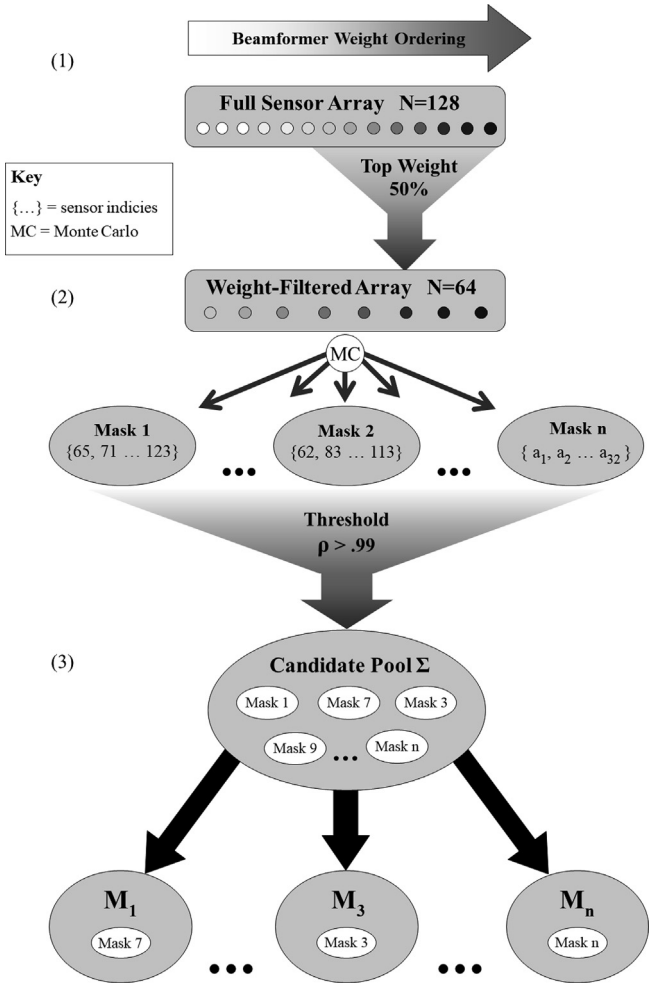

Fig. 2. An overview of the 3-step Monte Carlo dimensionality reduction approach. (1) Each h-EEG sensor is assigned a beamformer weight vector and sensors in the top 50% of weights are selected for Monte Carlo sampling. (2) The Monte Carlo sampling algorithm randomly generates a set of 32-sensor masks from the pool of high-weight sensors. (3) Masks that produce time-series which show a 0.99 correlation (ρ) with the original 128-sensor NF time-series are then selected to create Candidate Pool Σ. A wide variety of user- and protocol-specific criteria can be used to further refine Σ into a set of idealized montage pools, M.

2.2.1. Beamformer-weight based reduction

As an optimization step to the MC sampling process, we began by quickly eliminating unimportant sensors from the configuration space. As a measure of sensor importance, the Euclidean norm of each sensor's beamformer weight vector was calculated. The sensors with the 64 lowest normed beamformer magnitudes were presumed to have a small influence on the feedback signal and so were then excluded from the pool of sensors which would be used to generate the 32-sensor montages. By randomly generating 32-sensor montages from a pool of 64 sensors rather than 128 the number of potential montages in Ω is reduced by half. Note that while this optimization step is optional, it reduces the computational resources necessary for sensor reduction.

2.2.2. Monte Carlo sampling

Monte Carlo sampling was used to randomly generate three thousand 32-sensor montages for each raw EEG datafile in the testing set ($n = \sim 1386$). These montages were randomly created by using a Mersenne Twister pseudo-random generator algorithm (Matsumoto and Nishimura, 1998; Rubinstein and Kroese, 2016) to select 32-sensors from the 64-sensors configuration space. Each generated montage was associated with one of the 1386 raw EEG data files and all subsequent montage performance testing was done using the data in its associated parent file.

After montage generation, a ground truth NF time series was generated for each parent datafile using the original full 128-sensor montage. This time series was generated by first applying an LCMV beamformer mask (the same used in Section 2.1) targeting the PCC. A bandpass filter was then used to extract the gamma band signal from the beamformed data. This data was then average-referenced and divided into one second epochs. Within each epoch, the gamma band signal power was averaged and smoothed using a half-gaussian filter. This produced a single NF time series which was identical to that which the recorded participant received.

This same process was then used to generate a NF time series for each of the 32-sensor montages. Each montage's time series was calculated using the raw EEG data from its parent datafile and the LCMV weight of its 96 unused sensors were set to zero.

For every 32-sensor montage a Pearson correlation, ρ, was calculated between the 32-sensor time series it produced and the full 128-sensor time series associated with its parent datafile. This way we obtained a single ρ for each instance from the 32-sensor generated montage pool. ρ was used as a measure of montage reliability. Montages with an associated $\rho > 0.99$ were considered "high-performing" and were added to the high-performing montage pool Σ.

2.2.3. Montage selection refinement

Once Σ is created, a wide variety of refinement techniques can be used to produce further optimized montages. For our purposes, we created two different refined montage pools M_f and M_k from Σ. M_f contains a single montage and was generated by selecting the 32 most commonly occurring sensor locations in Σ. M_k contains multiple montages each generated by using different seeding parameters with a 4-dimensional k-means clustering algorithm to analyze Σ.

The k-means clustering analysis was performed using the Armadillo C++ Library (Sanderson, 2010). The first three dimensions were the x, y, z coordinates of the sensor's location and the fourth dimension was the sensor's selection status (a weighting value of 1 was given for selected sensors and 0 for unselected sensors). The static spread seeding parameter was used for seed initialization. The target number of clusters for this function was experimentally determined to be ~45, so that at least 32 major clusters were produced. Each run output a normalized array of sensor coordinates and an associated cluster probability value ranging between 0 and 1. The sensor coordinates associated with the top 32 cluster probabilities were then selected to create each M_k montage.

2.3. Evaluation of refined montage performance

Until this step, montage performance has only been evaluated using a single datafile. In order to accurately reflect montage performance against a diverse, real-world population, certain select montages were tested against every datafile in the testing set. Population-wide testing was performed for each selected montage by following the time series generation procedure outlined in Section 2.2.2, and then calculating the Pearson correlations between the candidate 32-sensor montage every 128-sensor time series generated from the parent testing datasets. This produced a set of 1386 ρ values for each montage which was plotted as a histogram. Various graph statistics were then calculated for montage performance comparison.

The montages selected for population-wide performance testing were M_f, M_k, and a single representative montage from Σ. Addi-

tionally, one montage generated using the optional beamformer reduction step (Section 2.2.1) and one montage produced without beamformer reduction were tested in this manner. Both of these montages had a ρ value of 0.0 and their results were used to explore the effects of the beamformer reduction step.

3. Results

3.1. Impact of beamformer weight reduction

The MC simulation produced about 4 million 32-sensor montages. These montages produced a skewed distribution of ρ values (see "Beamformer Weighted" line, Fig. 3). Application of the beamformer-weight based reduction significantly increased the median ρ value of montages generated by MC simulation (see Fig. 3). The median of the non-beamformer reduced dataset was 0.68 while the median of the beamformer-weight reduced dataset was 0.79.

3.2. Creation of Σ

After evaluating all the montages generated by MC sampling, Σ contained a total of ~4500 unique montages each with a $\rho > 0.99$. To illustrate the quality of NF signals produced by montages in Σ, a representative time-series plot with ρs belonging to various correlation percentiles can be seen in Fig. 4. A time-series plot, illustrating the quality of NF signals produced by montages in Σ with representative values of ρ belonging to various correlation percentiles is illustrated in Fig. 4.

3.3. Refined montage performance

The histograms for each of the five montages selected for population-wide testing can be seen in Fig. 5. The 0.0 ρ montages demonstrate that the beamformer weight reduction step significantly increased the montages' median population-wide ρ values. The median of the non-beamformer reduced graph was 0.39, while that number increased to 0.67 for the beamformer weight reduced montage (Fig. 5a and b). The single 0.99 ρ montage selected from Σ slightly out-performed the machine learning montage, M_k (Fig. 5c and d). The statistically selected montage, M_f, had the highest population-wide performance and could reproduce the original NF signal with a $\rho > 0.80$ on 72% of the parent datasets. Summary statistics for each graphs' performance and distribution can be seen in Table 1. Since ρ is selected to be 0.99 the p-value is 0.01.

4. Discussion

In the present work, we used a multistep approach to EEG sensor reduction that allowed us to reliably reproduce an h-EEG NF measure on a l-EEG system. This work is one of the first attempts to establish a translational pathway which enables h-EEG developed NF measures to be implemented on clinically and commercially accessible l-EEG systems. Prior work on EEG sensor

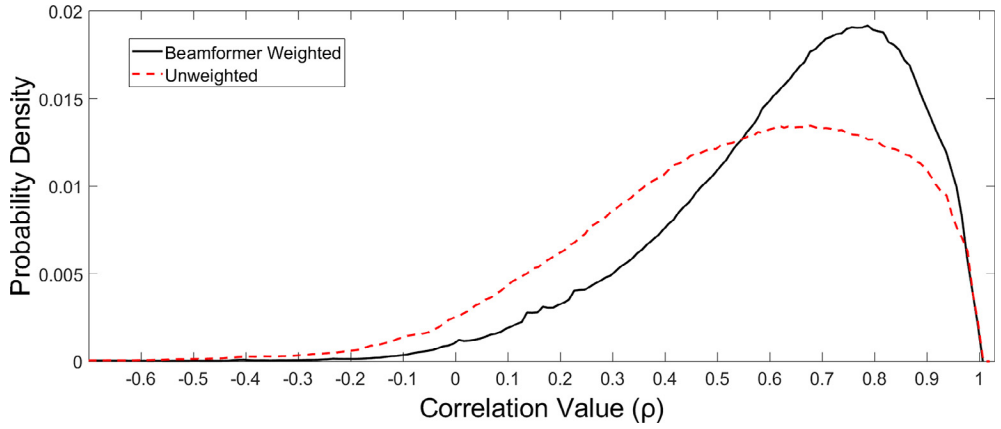

Fig. 3. Probability distribution of the correlation values between signal obtained from 32-sensor montage (from MC simulation) and that from 128-sensor full montage (solid line). The same simulation without beam-former weight based filter (dashed line).

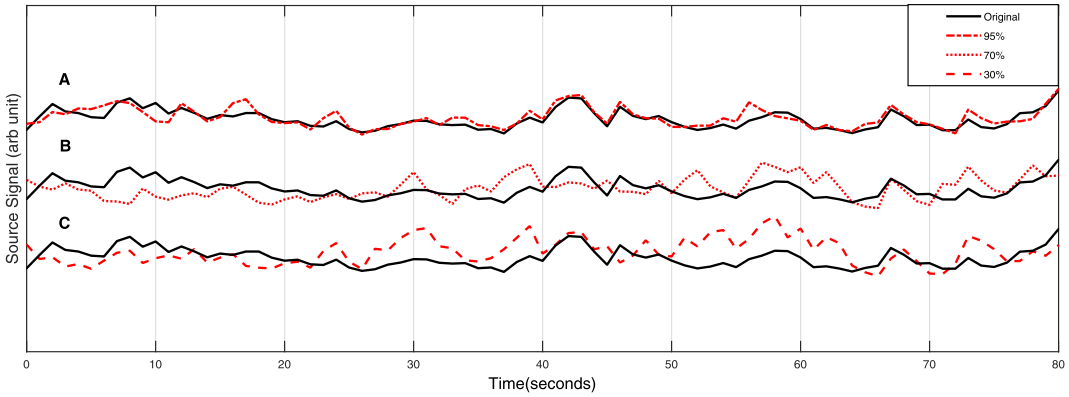

Fig. 4. Comparison between NF time series produced from an original 128-sensor dataset (solid line) and those derived from three montage-produced time series representing different degrees of correlation (a, b, and c)].

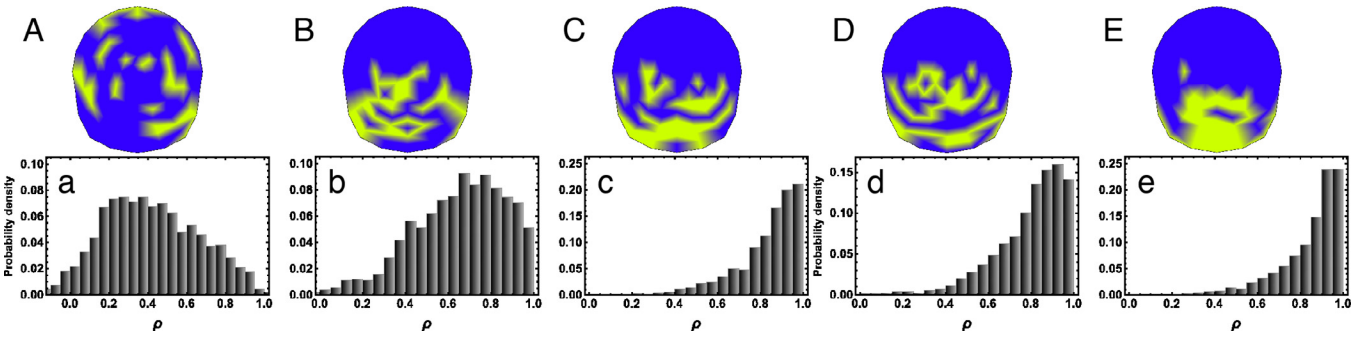

Fig. 5. Spatial masks showing scalp sensor locations of representative montages' (yellow) (A–E). (a) Correlation distribution produced by a low-correlation (ρ = 0.0) 32-sensor montage generated with no beamformer reduction filtering (b) Correlation distribution produced by a low-correlation (ρ = 0.0) 32-sensor montage generated with beamformer reduction filtering. (c) Correlation distribution produced by 32-sensor montage chosen from high-correlation pool Σ (ρ = 0.99) (d) Correlation distribution produced by montage generated using k-means clustering analysis on Σ (M_k) (e) Correlation distribution produced by montage comprised of the 32 most commonly appearing sensors in Σ (M_f). (For interpretation of the references to color in this figure legend, the reader is referred to the web version of this article.)

Table 1
Quantitative summary of the distributions in Fig. 5.

Distribution	Median	Percent of data above:		
		$\rho > 0.70$	$\rho > 0.80$	$\rho > 0.95$
5a	0.39	14%	7%	2%
5b	0.67	45%	28%	12%
5c (Σ)	0.88	83%	69%	41%
5d (M_k)	0.83	76%	59%	30%
5e (M_f)	0.89	85%	72%	48%

reduction has focused primarily on the detection of epileptiform signals and has been limited to EEG systems with fewer than ~70 electrodes (Machado et al., 2018; Pellegrino et al., 2016; Herta et al., 2017). In contrast, the currently presented sensor reduction method is highly adaptable and could be tailored for use with EEG systems of any size and any target brain region (e.g. NF for ADHD, motor cortex activation, epileptiform signal detection).

The key component of this method was the use of Monte Carlo sampling to query a large search space as well as eliminate human biases. Monte Carlo sampling enabled the nearly infinite number of potential 32-sensor montage configurations to be explored in an efficient and systematic way. The Monte Carlo analysis was able to reach an asymptotically convergent outcome by sampling a miniscule portion (~$2E^{-11}$ percent) of the total configuration space (Fig. 3). From this small sample we were able to produce 4500 reduced-sensor masks (Σ) which were capable of generating NF nearly identical to that of the original 128-sensor montage. This high output-to-sampling ratio suggests there are potentially millions of additional montages which could be generated to meet Σ's high reliability threshold.

The beamformer-weight based reduction greatly improved the odds of generating high-correlation montages. Specifically, discarding the lowest 50% of sensors increased the likelihood of generating a high-correlation montage by ~25% (Fig. 3). It is important to note that beamformer-weight reduction is optional for this sensor reduction method, and it only serves to increase the efficiency of high-correlation montage generation. h-EEG measures that do not use source targeting can still be adapted to Monte Carlo sampling reduction, however, the process will be less computationally efficient.

Most importantly, montages generated by our reduction method were able to reproduce the original h-EEG NF signal with high accuracy. Even without refinement, a randomly selected montage from Σ maintained ρ values above 0.8 for ~69% of the population-wide dataset (Fig. 5c). Other unrefined montages in Σ were also tested and appeared to show similar performance. These findings indicate that even without the use of refinement steps (like machine learning analysis) the Monte Carlo sensor reduction strategy can produce reduced montages which may be suitable for many commercial level applications.

In clinical settings where high reliability is paramount, the use of a refinement process is ideal. Both of our refinement processes, M_f and M_k, substantially increased NF signal reliability. While M_f produced the most reliable NF signal (Table 1), it's physical montage distribution (Fig. 5E) might be challenging to implement in certain clinical scenarios. In situations where physical cap design restrictions exist, then using a more flexible refinement parameter like M_k might be ideal. The seeding parameters of M_k's k-means clustering algorithm can be tailored to accommodate a variety of spatial design preferences allowing M_k to serve as a compromise between design criteria and montage reliability.

Though we created 32-sensor montages for this study, it is still possible to generate montages of an even smaller size that can maintain high reliability. In our preliminary pilot analysis, we were able to use the Monte Carlo method to generate montages as small as 20 sensors and still produce montages with ρ values that could meet Σ's reliability threshold. Further sensor reduction was also supported by the k-means algorithm which indicated that around 25% of the 32 montage sensors appeared to have minimal influence on correlational outcomes. However, the Monte Carlo method produced high quality montages at a much lower occurrence rate as the target montage size decreased. This significantly increased the amount of computational time necessary to create a Σ pool large enough for use with refinement techniques. Thus, when using this Monte Carlo sensor reduction method, it is important to consider trade-offs between target montage size and computational power necessary to produce a desired montage.

When performing EEG sensor reduction, another important consideration is to determine at what ρ value the efficacy of the output signal begins to degrade. In the case of NF, the efficacy of therapy is dependent on the user's perception and interpretation of the feedback signal. This suggests that inconsistencies in the NF signal which are unnoticeable to the user have little impact on NF efficacy. To our knowledge, no studies have examined the role of NF signal quality on therapeutic outcomes. The qualitative visual similarities between the original signal and our reduced-sensor NF time series, even when the actual correlation between them is ρ = 0.70 (Fig. 4), suggest that such discrepancies may be clinically irrelevant if they are unnoticeable by users. Alternatively, it may be the case that such signal differences would lead to different clinical outcomes even if subjects were not aware of, or could not consciously perceive, any infidelities in the reduced-sensor sig-

nal. Testing this hypothesis would require an advanced neurophenomenological approach (Garrison et al., 2013; van Lutterveld et al., 2017) and is a good candidate for future research.

This sensor reduction method is highly flexible, and its use is not limited to only reducing h-EEG systems or NF measures. This sensor reduction method can be applied to EEG systems with any number of base electrodes and can be used to create specialized montages for the detection of any target brain activity. The flexibility of this sensor reduction method is possible because it is based solely on statistical sampling and correlational methods. With further testing, this automated sensor reduction method may prove ideal for sensor reduction in all varieties of EEG systems and may begin to enable the development of personalized EEG caps.

Although this proof-of-concept was performed on an h-EEG NF system, it can be used to increases the applicability, accessibility, and reliability of a wide variety of EEG feedback and detection systems. This method creates a translational pathway which allows us to utilize the superior accuracy and robustness of h-EEG systems while still maintaining the flexibility and cost-effectiveness of l-EEG systems. Future work on EEG sensor reduction will only continue to streamline and improve this process.

One potential limitation of our method is that the outcome is sensitive to the choice and size of the targeted brain region. For larger regions of interest, the distribution and redundancy of the reduced-sensors over the scalp may not necessarily produce a well-defined regionally clustered set as reported in this article. The final design choice of the reduced-sensor cap would be heavily influenced by the distribution of the montage pool candidates over the scalp. Additionally, our results are potentially limited by the chosen frequency band of interest. High frequency bands of interest as we reported in this study may be focal and not spread over large cortical regions if these techniques are applied in other settings. Another limitation is computation costs associated with unconstrained MC sampling. A more efficient approach would be adaptive sampling such that the sensors with greater beamformer weight would be sampled with higher frequencies to make faster convergence and minimize unimportant sampling. Such an efficient approach would be useful if we need absolute minimum number of reduced-sensors instead of 32-sensors montages described in this study.

5. Conclusion

A new EEG sensor reduction method was used to accurately reduce a 128-sensor NF system into a 32-sensor NF system. This method utilized a Monte Carlo sampling strategy to systematically explore the entire set of potential 32-sensor montages and was able to produce thousands of montages which could reproduce the 128-sensor NF with high accuracy. This sensor reduction method could be applied to EEG systems of any size and target signal. Future studies could build on this method by increasing the computational efficiency and quality of the montage generation process, and by performing additional proof-of-concept studies on EEG systems of different types and sizes.

Acknowledgements

We thank Dr. Alex Ossadtchi, Dr. Mark Pflieger, and Dr. Corey S. O'Hern for helpful advice, Stephanie Noble, Socheata Poeuv, Phil Murray, Shenil Dodia, Pranav Maddi, Akschi Haggenmiller and Cinque McFarlane-Blake for helping with the initial exploratory setup, Yale Office of Collaborative Research for facilitation of collaboration, Bridge Builders Associates for seed funding to GoBlue Labs (now Claritas Mindsciences). We thank the Yale University Faculty of Arts and Sciences High Performance Computing Center and the University of Massachusetts Medical School Green High Performance Computing Facility for providing computational resources.

Funding

This work was supported by a grant from the Fetzer Trust.

Conflict of interest statement

Yale University has filed for patent protection of the application of providing neurofeedback from the PCC. Drs. Brewer and Pal own stock in a company that has rights to license this patent. No other authors have potential conflicts of interest.

Appendix A. Supplementary material

Supplementary data to this article can be found online at https://doi.org/10.1016/j.clinph.2018.11.023.

References

Acar, Akalin Zeynep, Makeig Scott. Effects of forward model errors on EEG source localization. Brain topography 2013:378–96.
Anderson S. On optimal dimension reduction for sensor array signal processing. Signal Process 1993;30:245–56.
BioSemi BV. BioSemi ActiveTwo [EEG system]. Amsterdam: BioSemi; 2011.
Chu CJ. High density EEG—What do we have to lose? Clin Neurophysiol 2015;126:433–4. https://doi.org/10.1016/j.clinph.2014.07.003.
Friedman JH. On bias, variance, 0/1—loss, and the curse-of-dimensionality. Data Min Knowl Discov 1997;1:55–77. https://doi.org/10.1023/A:1009778005914.
Garrison KA, Scheinost D, Worhunsky PD, Elwafi HM, Thornhill TA, Thompson E, et al. Real-time fMRI links subjective experience with brain activity during focused attention. Neuroimage 2013;81:110–8. https://doi.org/10.1016/j.neuroimage.2013.05.030.
Greenblatt RE, Ossadtchi A, Pflieger ME. Local linear estimators for the bioelectromagnetic inverse problem. IEEE Trans Signal Process 2005;53:3403–12. https://doi.org/10.1109/TSP.2005.853201.
Herta J, Koren J, Fürbass F, Hartmann M, Gruber A, Baumgartner C. Reduced electrode arrays for the automated detection of rhythmic and periodic patterns in the intensive care unit: frequently tried, frequently failed? Clin Neurophysiol 2017;128:1524–31. https://doi.org/10.1016/j.clinph.2017.04.012.
Jatupaiboon N, Pan-ngum S, Israsena P. Real-time EEG-based happiness detection system. Sci World J 2013. https://doi.org/10.1155/2013/618649.
Jiang S, Zhou P, Li Z, Li M. Emotion-driven lifelogging with wearables. In: IEEE conference on computer communications workshops. p. 1091–2.
Keogh E, Mueen A. Curse of dimensionality. In: Encyclopedia of machine learning. Springer; 2011. p. 257–8.
Lubar JF, Swartwood MO, Swartwood JN, O'Donnell PH. Evaluation of the effectiveness of EEG neurofeedback training for ADHD in a clinical setting as measured by changes in TOVA scores, behavioral ratings, and WISC-R performance. Biofeedback Self Regul 1995;20:83–99. https://doi.org/10.1007/BF01712768.
Machado A, Cai Z, Pellegrino G, Marcotte O, Vincent T, Lina JM, et al. Optimal positioning of optodes on the scalp for personalized functional near-infrared spectroscopy investigations. J Neurosci Methods 2018;309:91–108. https://doi.org/10.1016/j.jneumeth.2018.08.006.
Matsumoto M, Nishimura T. Mersenne twister: a 623-dimensionally equidistributed uniform pseudo-random number generator. ACM T Model Comput S 1998;8:3–30. https://doi.org/10.1145/272991.272995.
Mihajlović V, Grundlehner B, Vullers R, Penders J. Wearable, wireless EEG solutions in daily life applications: what are we missing? IEEE J Biomed Health Inform 2015;19:6–21. https://doi.org/10.1109/JBHI.2014.2328317.
Niha K, Banu WA. Brain signal processing: technologies, analysis and application. In: 2016 IEEE international conference on computational intelligence and computing research (ICCIC). p. 1–6.
Pal P, O'Hern CS, Blawzdziewicz J, Dufresne ER, Stinchcombe R. Minimal model for kinetic arrest. Phys Rev E Stat Nonlin Soft Matter Phys 2008;78:011111. https://doi.org/10.1103/PhysRevE.78.011111.
Pellegrino G, Machado A, von Ellenrieder N, Watanabe S, Hall JA, Lina JM, et al. Hemodynamic response to interictal epileptiform discharges addressed by personalized EEG-fNIRS recordings. Front Neurosci 2016;10:102. https://doi.org/10.3389/fnins.2016.00102.
Peniston EG, Kulkosky PJ. Alpha-theta brainwave neuro-feedback for Vietnam veterans with combat-related post-traumatic stress disorder. Med Psychother 1991;4:47–60.
Rubinstein RY, Kroese DP. Simulation and the Monte Carlo method. John Wiley & Sons; 2016.
Sanderson C Armadillo. An open source C++ linear algebra library for fast prototyping and computationally intensive experiments. NICTA; 2010. p. 1–15.

Sterman MB, Egner T. Foundation and practice of neurofeedback for the treatment of epilepsy. Appl Psychophysiol Biofeedback 2006;31:21–35. https://doi.org/10.1007/s10484-006-9002-x.

Stytsenko K, Jablonskis E, Prahm C. Evaluation of consumer EEG device Emotiv EPOC. MEi: CogSci conference, Ljubljana, 2011.

Surangsrirat D, Intarapanich A. Analysis of the meditation brainwave from consumer EEG device. In: SoutheastCon 2015. p. 1–6.

Thibault RT, Lifshitz M, Raz A. The self-regulating brain and neurofeedback: experimental science and clinical promise. Cortex 2016;74:247–61. https://doi.org/10.1016/j.cortex.2015.10.024.

van Lutterveld R, Houlihan SD, Pal P, Sacchet MD, McFarlane-Blake C, Patel PR, et al. Source-space EEG neurofeedback links subjective experience with brain activity during effortless awareness meditation. Neuroimage 2016;151:117–27. https://doi.org/10.1016/j.neuroimage.2016.02.047.

van Lutterveld R, van Dellen E, Pal P, Yang H, Stam CJ, Brewer J. Meditation is associated with increased brain network integration. Neuroimage 2017;158:18–25. https://doi.org/10.1016/j.neuroimage.2017.06.071.

Wu X, Liou S. Mindfulness biofeedback interface (MBI) design: Challenges and opportunities. In: International conference on orange technologies, ICOT 2015. p. 153–6.